

Twinned tetragonal structure and equation of state of NaTh_2F_9

Andrzej Grzechnik^{a,*}, Wolfgang Morgenroth^{b,c}, Karen Friese^a

^a*Departamento de Física de la Materia Condensada, Universidad del País Vasco, Bilbao, Spain*

^b*Institut für Anorganische Chemie, Georg-August-Universität, Göttingen, Germany*

^c*Department of Chemistry, Aarhus University, Denmark*

Received 5 November 2007; received in revised form 17 January 2008; accepted 18 January 2008

Available online 15 February 2008

Abstract

The crystal structure and stability of NaTh_2F_9 have been studied using thermal analysis, powder X-ray diffraction at atmospheric conditions, and single-crystal X-ray diffraction at high pressure. Sodium dithorium fluoride is stable at least up to 5.0 GPa at room temperature and to 954 K at ambient pressure. In contrast to earlier investigations, which have reported the structure to be cubic ($I\bar{4}3m$, $Z = 4$), we observe a tetragonal distortion of the lattice. The actual crystal structure ($I\bar{4}2m$, $Z = 4$) is twinned and composed of corner-sharing distorted ThF_9 tricapped trigonal prisms and distorted NaF_6 octahedra. The twinning element is a three-fold axis from cubic symmetry. The ThF_9 polyhedra are rigid and it is the volume changes of the octahedra around the Na atoms that have the major contribution to the bulk compressibility. The zero-pressure bulk modulus B_0 and the unit-cell volume at ambient pressure V_0 are equal to 99(6) GPa and $663.1(1.0) \text{ \AA}^3$, respectively, with the fixed first pressure derivative of the bulk modulus $B' = 4.00$. An inspection of the known crystalline phases in the system NaF-ThF_4 reveals that their bulk moduli increase with the increasing ThF_4 content.

© 2008 Elsevier Inc. All rights reserved.

Keywords: Complex thorium fluorides; Crystal structure; High pressure; X-ray diffraction

1. Introduction

Complex fluorides of actinides are considered for nuclear applications as fuels in molten salt reactors and as solvents for spent nuclear solid fuel [1–4]. Some of the most important systems contain NaF and ThF_4 components. To construct and use a reactor, it is important to know structural, physical, and thermodynamical properties of the materials. This includes not only their phase diagrams and the conditions at which they are (un)stable but also their equations of state.

The ThF_8 coordination polyhedron in solid ThF_4 is a square antiprism [5,6]. In complex fluorides, the Th coordination number is either 8 (a dodecahedron, a square antiprism, or a bicapped trigonal prism) [5,7–9] or 9 (a tricapped trigonal prism) [5,10,11]. Based on X-ray powder diffraction data, the crystal structure of NaTh_2F_9 sodium dithorium fluoride was determined to be of the U_2F_9 type ($I\bar{4}3m$, $Z = 4$) [12,13]. The fluorine atoms were located

by spatial considerations and the coordination number of the Th atoms was assumed to be 9. Since it was not possible to place four Na atoms in a unit cell in accordance with the $I\bar{4}3m$ space group symmetry, the Na atoms were inserted in the partially occupied octahedral sites $6b$ [13].

Here in this study, we have re-determined the crystal structure of NaTh_2F_9 and have investigated its stability using thermal analysis, powder X-ray diffraction at atmospheric conditions, and single-crystal X-ray diffraction at high pressure. Our results are discussed in comparison to those for $\beta\text{-Na}_2\text{ThF}_6$ [11], another crystalline phase in the condensed NaF-ThF_4 system [12–14].

2. Experimental

A single crystal of NaTh_2F_9 was synthesized with the Czochralski method. A part of it was ground for thermal analysis and powder X-ray diffraction experiments.

Differential scanning calorimetry was performed using the systems Pyris 1 and 7 (Perkin-Elmer) in the temperature range from 290 to 954 K.

*Corresponding author. Fax: +34 94 601 35 00.

E-mail address: andrzej@wm.lc.ehu.es (A. Grzechnik).

A powder X-ray diffraction experiment at room temperature and ambient pressure was carried out at the *D3* Beamline in HASYLAB (Hamburg, Germany), $\lambda = 0.47686 \text{ \AA}$, equipped with a marCCD165 detector. The sample was contained in a 0.3 mm glass capillary. The two-dimensional image was integrated with the program FIT2D to yield an intensity versus 2θ diagram [15].

Single-crystal measurements were performed using a diffractometer IPDS-2 T (STOE) with the $\text{MoK}\alpha$ radiation. A series of experiments at high pressures was carried out in the Ahsbahs-type diamond anvil cell (the opening angle of 90°) [16]. The diamond culets ($600 \mu\text{m}$) were modified by laser machining so that the angle between them and the tapered parts of the diamonds was 40° . A $250 \mu\text{m}$ hole was drilled into a stainless steel gasket preindented to a thickness of about $80 \mu\text{m}$. The intensities were collected upon compression. They were indexed, integrated, and corrected for absorption using the STOE software.¹ Shaded areas of the images by the diamond anvil cell were masked prior to integration. The intensities were integrated simultaneously with three orientation matrices, corresponding to the crystal of NaTh_2F_9 , and to the two diamonds of the cell. Due to their hemispherical shape, no absorption correction was necessary for the diamond anvils.² Ruby luminescence method [17] was used for pressure calibration and the 1:4 mixture of ethanol:methanol was used as a hydrostatic pressure medium.

3. Results and discussion

The results of thermal analysis indicate that NaTh_2F_9 does not undergo any phase transition in the temperature range 290–954 K.

Fig. 1 shows a powder X-ray pattern of NaTh_2F_9 measured at ambient conditions. Several split reflections cannot be accounted for with cubic symmetry [13]. This suggests that the true space group is a non-cubic subgroup of $I\bar{4}3m$. Consequently, the measured diagram was refined with different space groups using the Le Bail method implemented in the program JANA2000 [18] (Fig. 1). Of the two maximal subgroups $R3m$ and $I\bar{4}2m$ of space group $I\bar{4}3m$, the fit with symmetry $I\bar{4}2m$ is superior and explains all the observed reflections. The refined lattice parameters and unit-cell volume in space group $R3m$ are $a = 12.371(1) \text{ \AA}$, $c = 7.478(3) \text{ \AA}$, and $V = 991.1(3) \text{ \AA}^3$. In space group $I\bar{4}2m$, they are $a = 8.763(1) \text{ \AA}$, $c = 8.640(2) \text{ \AA}$, and $V = 663.5(2) \text{ \AA}^3$. Further symmetry lowering to the orthorhombic system does not improve the fit significantly and the refined lattice parameters do not deviate from the tetragonal ones within estimated standard deviations.

¹X-Area and X-Shape. STOE & Cie GmbH, Darmstadt.

²Further details of the crystallographic investigations can be obtained from the Fachinformationszentrum Karlsruhe, D-76344 Eggenstein-Leopoldshafen, Germany, on quoting the depository numbers CSD 419215-419219.

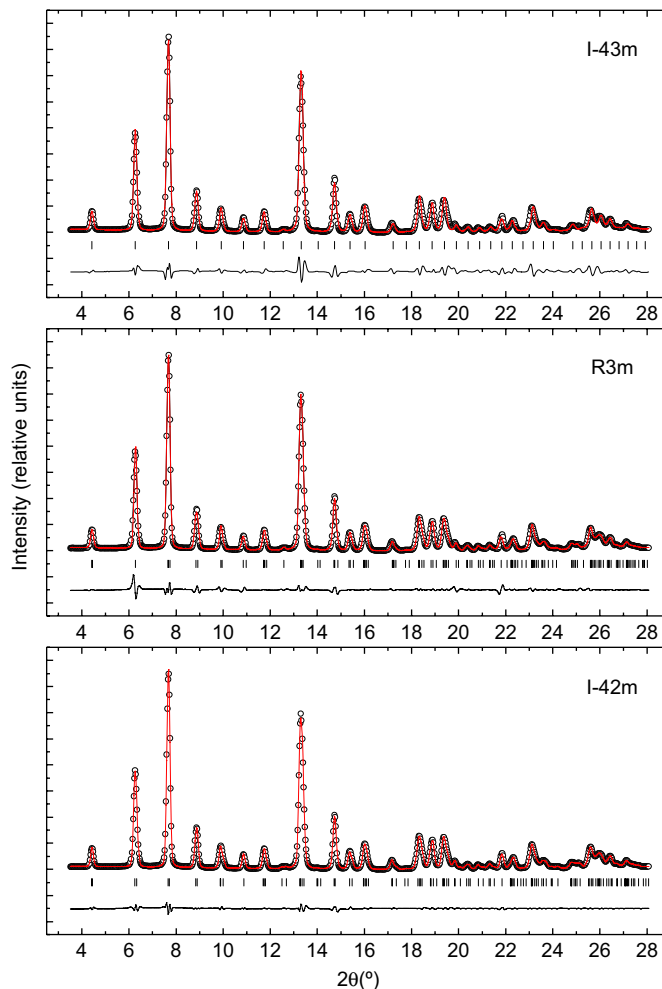


Fig. 1. Observed powder diagram (black circles) compared with the calculated (red lines) and difference (black lines) diagrams obtained using the Le Bail method [18] in space groups $I\bar{4}3m$, $R3m$, and $I\bar{4}2m$ (ambient conditions, $\lambda = 0.47686 \text{ \AA}$). Vertical markers indicate the positions of the calculated Bragg reflections.

Table 1 compares various structural models obtained from the refinements [18] of the single-crystal data measured at ambient conditions. In each case, the thermal displacement parameters for all the atoms were refined anisotropically. Two cubic models with space group symmetries $I\bar{4}3m$ and $I23$ were considered. While the first of them was a single-crystal model, the second one was a twinned one with a four-fold axis from the higher cubic symmetry as a twin element. Both models led to fairly high internal *R*-values. Final overall agreement factors are slightly lower for the $I23$ structure. Both cubic models have negative displacement parameters of individual atoms. The refined twin volume fractions in $I23$ do not show significant deviations from the ratio 1/2:1/2.

A rhombohedral model in $R3m$, which incorporated the four-fold axis of the cubic system as a twin element, also led to high internal *R*-values. The final agreement factors are similar to the ones for the cubic refinements, however, the displacement parameters of even more atoms turn

Table 1
Details of different refinements for a single crystal of NaTh₂F₉ at ambient conditions

Space group	$R(\text{int})_{\text{obs/all}}$	No. refl. _{obs/all}	Redundancy	R_{obs}	wR_{obs}	No. pars
$I\bar{4}3m^a$	14.93/14.93	240/240	17.16	3.91	5.16	17
$I23^b$	14.87/14.88	386/387	10.64	3.39	4.00	19
$I\bar{4}2m$	7.43/7.49	1088/1143	3.06	2.69	3.14	36
$R3m^c$	14.11/14.14	864/886	4.65	3.84	4.28	51
$I222$	7.43/7.49	1088/1143	3.60	2.70	3.14	60

No. refl. and No. pars are the number of unique reflections and the number of parameters, respectively. The total number of reflections (obs/all) is 3716/4117. All agreement factors are given in %.

^aThermal displacement parameters for F1 are negative.

^bThermal displacement parameters for Na and F1 are negative.

^cThermal displacement parameters for Th₂, F1, F2, and F3, F4, Na are negative.

negative. The twin volume fractions of the four individuals are approximately 0.35:0.29:0.14:0.22.

The tetragonal model in space group $I\bar{4}2m$, with the three-fold axis from the cubic system as a twin element, gives considerable lower internal R -values and the final agreement factors are significantly better than for the cubic and rhombohedral symmetries. All thermal displacement parameters are positive. It is remarkable, that the twin volume fractions deviate significantly from the ideal proportion of 1/3:1/3:1/3 with refined values of 0.653(8):0.033(7):0.31(4).

Finally, we tried a model with $I222$ symmetry assuming a combination of the three-fold and four-fold axes as twinning elements. This model basically yields identical final agreement factors as the ones obtained for the tetragonal model, although the number of parameters is increased to 60 (compared to 36 in the tetragonal model). The refined twin volume fractions give the same result as for the tetragonal symmetry with only three significant volume fractions corresponding to the three individuals related by the three-fold axis.

On the basis of these observations, we exclude the cubic and rhombohedral structures as plausible candidates for the crystal structure of NaTh₂F₉. This decision is supported by the powder diffraction data, which are in accordance neither with cubic nor with rhombohedral metrics (Fig. 1). Also, in view of the fact that the orthorhombic model does not improve the fit further, we are confident that the tetragonal twin model represents the correct choice. This model was also used for the refinement of the high-pressure data (Table 2). Indexing of the high-pressure single-crystal data does not show any indication for a further orthorhombic distortion of the metrics.

There are two possible sites for the Na atoms in space group $I\bar{4}2m$ ($4c$ and $2b$) obtained from the splitting of the Wyckoff position $6b$ in space group $I\bar{4}3m$, initially considered for NaTh₂F₉ [13]. Consequently, two structural models could be constructed by distributing the sodium atoms in different ways. The refinement of the model, in which both sites are partially occupied, leads to an occupancy at the site $2b$ practically equal to 0. In addition, the calculated bond valences, assuming that both sites are

Table 2
Experimental data for the single-crystal measurements ($I\bar{4}2m$, $Z = 4$)²

	0.0001 GPa	1.50 GPa	2.35 GPa	2.55 GPa	5.00 GPa
<i>Crystal data</i>					
a (Å)	8.763(1)	8.752(3)	8.743(4)	8.736(3)	8.672(3)
c (Å)	8.640(2)	8.534(3)	8.479(4)	8.471(3)	8.429(2)
V (Å ³)	663.5(2)	653.7(7)	648.1(9)	646.5(7)	633.9(6)
ρ (g cm ⁻³)	6.586	6.684	6.742	6.759	6.893
μ (mm ⁻¹)	44.964	45.636	46.027	46.144	47.061
<i>Data collection</i>					
No. meas. refl.	3716	826	750	766	832
Range of hkl	$-12 \leq h \leq 12$	$-7 \leq h \leq 8$	$-8 \leq h \leq 8$	$-6 \leq h \leq 6$	$-6 \leq h \leq 7$
	$0 \leq k \leq 12$	$0 \leq k \leq 7$	$0 \leq k \leq 7$	$0 \leq k \leq 8$	$0 \leq k \leq 8$
	$0 \leq l \leq 12$	$0 \leq l \leq 8$	$0 \leq l \leq 8$	$0 \leq l \leq 8$	$0 \leq l \leq 8$
No. obs. refl. ^a	1088	224	198	197	207
$R(\text{int})_{\text{obs}}$ ^b	7.43	6.71	7.04	7.73	7.91
$\sin(\theta)/\lambda$	0.7436	0.5041	0.5060	0.5064	0.5084
<i>Refinement</i> ^b					
R_{obs}	2.69	5.99	5.62	6.16	6.28
wR_{obs}	3.14	6.43	6.11	6.51	6.36
GoF _{obs}	1.95	2.69	2.51	2.64	2.74
No. parameters	36	16	16	16	16

^aCriterion for observed reflections is $|F_{\text{obs}}| > 3\sigma$.

^bAll agreement factors are given in %, weighting scheme $1/[\sigma^2(F_{\text{obs}}) + (0.01F_{\text{obs}})^2]$.

occupied by the Na atoms, are quite revealing. While the bond valence at the site $4c$ is nearly equal to 1, it is only about 0.7 at the $2b$ site. For these reasons, we believe that at ambient conditions the sodium atoms exclusively reside at the $4c$ site (Tables 1–3). However, it is quite likely that the actual Na distribution could be changed on heating and the $2b$ site may be occupied at high temperatures.

The $I\bar{4}2m$ structural model with the Na atoms solely at the $4c$ site was used for all the refinements of the high-pressure data (Tables 2 and 3), in which only the thermal displacement parameter of the Th atom was refined anisotropically. The thermal parameters for the Na, F1, F2, and F3, and F4 atoms were fixed to the respective isotropic thermal parameters of these atoms at ambient conditions (Table 3). The refined twin volume fractions are practically constant on compressing, suggesting that the

Table 3
Selected structural data from single-crystal refinements ($I\bar{4}2m$, $Z = 4$)

	0.0001 GPa	1.50 GPa	2.35 GPa	2.55 GPa	5.00 GPa
<i>Th atom (8i site)</i>					
<i>x</i>	0.18563(6)	0.1837(7)	0.1844(7)	0.1850(7)	0.1862(6)
<i>z</i>	0.8061(1)	0.8032(8)	0.8050(9)	0.8044(9)	0.8041(9)
U_{iso}	0.00962(9)	0.018(1)	0.0154(9)	0.021(1)	0.0200(8)
<i>Na atom (4c site)</i>					
U_{iso}	0.034(4)				
<i>F1 atom (8f site)</i>					
<i>x</i>	0.239(1)	0.262(6)	0.268(6)	0.277(6)	0.272(5)
U_{iso}	0.019(3)				
<i>F2 atom (4e site)</i>					
<i>z</i>	0.221(2)	0.199(12)	0.189(11)	0.193(11)	0.182(9)
U_{iso}	0.023(4)				
<i>F3 atom (16j site)</i>					
<i>x</i>	0.4525(8)	0.451(5)	0.451(5)	0.459(5)	0.460(4)
<i>y</i>	0.200(1)	0.179(8)	0.180(7)	0.176(6)	0.174(5)
<i>z</i>	0.801(1)	0.804(7)	0.790(5)	0.788(5)	0.789(4)
U_{iso}	0.022(2)				
<i>F4 atom (8i site)</i>					
<i>x</i>	0.2110(9)	0.224(5)	0.223(6)	0.222(6)	0.217(5)
<i>z</i>	0.546(1)	0.551(8)	0.555(7)	0.555(8)	0.546(6)
U_{iso}	0.021(3)				

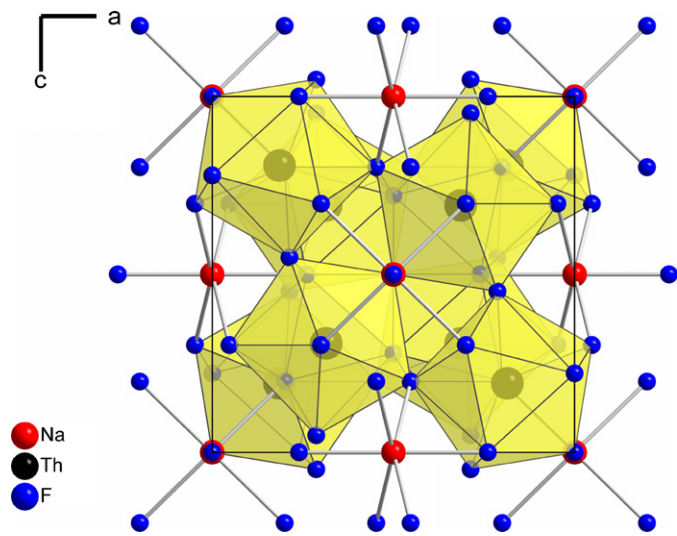


Fig. 2. Crystal structure of NaTh_2F_9 ($I\bar{4}2m$, $Z = 4$) at ambient conditions. The polyhedra around the Th atoms are drawn.

domain structure is not affected by decreasing the unit-cell volume.

The crystal structure of sodium dithorium fluoride ($I\bar{4}2m$, $Z = 4$) at ambient conditions is shown in Fig. 2. It is built of corner-sharing distorted ThF_9 tricapped trigonal prisms and distorted NaF_6 octahedra. Both F1 and F3 atoms are coordinated by two Th and one Na atoms. The F2 and F4 atoms are only connected to two Th atoms. Our results of this and a previous study [11] demonstrate that the nine-fold coordination of the Th atoms to fluorine atoms seems to be characteristic of the

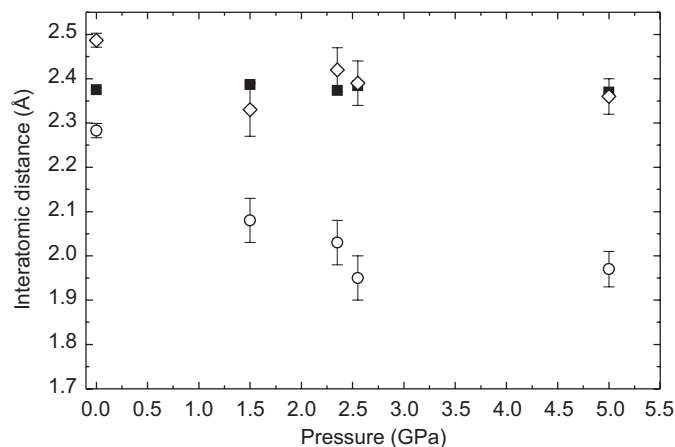


Fig. 3. Pressure dependence of interatomic distances. The full symbols represent the average Th-F distances in the ThF_9 tricapped trigonal prisms. The open symbols represent the Na-F distances in the NaF_6 octahedra.

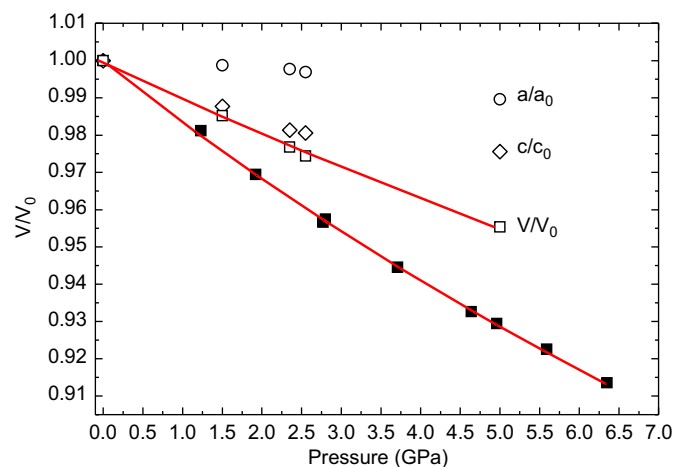


Fig. 4. Pressure dependence of the normalized lattice parameters and unit-cell volume in NaTh_2F_9 (open symbols) compared with the dependence of the normalized unit-cell volume in $\beta\text{-Na}_2\text{ThF}_2$ [11] (solid symbols). The lines are the Murnaghan equation-of-state fits to the compressibility data.

crystalline phases in the NaF-ThF_4 system, in which the ThF_8 coordination polyhedron in solid ThF_4 is a square antiprism [5,6].

Pressure dependence of interatomic distances Th-F and Na-F is shown in Fig. 3. Unlike the Na-F distances, the Th-F distances are essentially insensitive to increased pressure. Upon compression, the NaF_6 octahedra become more distorted as seen from the divergence of their Na-F1 apical and Na-F3 basal distances. This suggests that the polyhedral volume changes around the Na atoms have the major contribution to the bulk compressibility of this material.

The compressibility data (Table 2) for sodium dithorium fluoride shown in Fig. 4 could be fitted with the Murnaghan equation of state to give the zero-pressure bulk modulus B_0 and the unit-cell volume at ambient pressure V_0 (for the fixed first pressure derivative of the bulk modulus $B' = 4.00$) equal to 99(6) GPa and $663.1(1.0) \text{ \AA}^3$,

respectively. This material is more compressible along the shorter c -axis so that the c/a axial ratio decreases at high pressures. The larger bulk modulus of NaTh_2F_9 than that of $\beta\text{-Na}_2\text{ThF}_6$ ($B_0 = 58(1)\text{ GPa}$) [11] could be explained by a larger molar ratio of the ThF_4 and NaF components in NaTh_2F_9 (2:1) than in $\beta\text{-Na}_2\text{ThF}_6$ (1:2).

Acknowledgments

The single crystal of NaTh_2F_9 was grown by J.-Y. Gesland (Univ. Le Mans, France). We thank E. Bocanegra for the calorimetric measurements and one of the anonymous referees for pointing out the importance of a Hamilton test to us. AG and KF acknowledge the Gobierno Vasco, the Ministerio de Ciencia y Tecnología, and the European Science Foundation for supporting their high-pressure laboratory.

References

- [1] R.W. Moir, E. Teller, Nucl. Technol. 151 (2005) 334.
- [2] J.P.M. van der Meer, R.J.M. Konings, H.A.J. Oonk, J. Nucl. Mater. 357 (2006) 48.
- [3] Ch. Le Brun, J. Nucl. Mater. 360 (2007) 1.
- [4] J.P.M. van der Meer, R.J.M. Konings, J. Nucl. Mater. 360 (2007) 16.
- [5] A.F. Wells, Structural Inorganic Chemistry, fifth ed., Oxford University Press, Oxford, 1984.
- [6] G. Benner, B.G. Müller, Z. Anorg. Allg. Chem. 588 (1990) 33.
- [7] G. Brunton, Acta Cryst. B 27 (1971) 2290.
- [8] R.R. Ryan, R.A. Penneman, Acta Cryst. B 27 (1971) 829.
- [9] A. Cousson, M. Pagès, R. Chevalier, Acta Cryst. B 35 (1979) 1763.
- [10] G. Brunton, Acta Cryst. B 27 (1971) 1823.
- [11] A. Grzechnik, M. Fechtelkord, W. Morgenroth, J.M. Posse, K. Friese, J. Phys.: Condens. Matter 19 (2007) 266219.
- [12] W.H. Zachariasen, Acta Cryst. 1 (1948) 265.
- [13] W.H. Zachariasen, Acta Cryst. 2 (1949) 390.
- [14] R.E. Thoma, H. Insley, G.M. Hebert, H.A. Friedman, C.F. Weaver, J. Amer. Ceram. Soc. 46 (1963) 37.
- [15] A.P. Hammersley, S.O. Svensson, M. Hanfland, A.N. Fitch, D. Häusermann, High Press. Res. 14 (1996) 235.
- [16] (a) G.J. Piermarini, S. Block, J.D. Barnett, R.A. Forman, J. Appl. Phys. 46 (1975) 2774;
(b) H.K. Mao, J. Xu, P.M. Bell, J. Geophys. Res. 91 (1986) 4673.
- [17] (a) H. Ahsbahs, Z. Kristallogr. Suppl. 9 (1995) 42;
(b) H. Ahsbahs, Z. Kristallogr. 219 (2004) 305.
- [18] V. Petricek, M. Dusek, L. Palatinus, JANA2000. The crystallographic computing system. Institute of Physics, Praha, Czech Republic, 2000.